

THE SMALL-SCALE STRUCTURE OF MHD TURBULENCE IN HIGH-PRANDTL-NUMBER PLASMAS

ALEXANDER A. SCHEKOCIHIN, JASON L. MARON, STEVEN C. COWLEY

Plasma Physics Group, Imperial College, Blackett Laboratory, Prince Consort Rd., London SW7 2BW, England
a.schekochihin@ic.ac.uk, maron@tapir.caltech.edu, steve.cowley@ic.ac.uk

JAMES C. MCWILLIAMS

Department of Atmospheric Sciences, UCLA, Los Angeles, California 90095-1565
jcm@atmos.ucla.edu
27 March 2002

ABSTRACT

We study the intermittency and field-line structure of the MHD turbulence in plasmas with very large magnetic Prandtl numbers. In this regime, which is realized in the interstellar medium, accretion disks, and protogalaxies, magnetic fluctuations can be excited at scales below the viscous cutoff. The salient feature of the resulting small-scale magnetic turbulence is the folded structure of the fields. It is characterized by very rapid transverse spatial oscillation of the field direction, while the field lines remain largely unbent up to the scale of the flow. Quantitatively, the fluctuation level and the field-line geometry can be studied in terms of the statistics of the field strength and of the field-line curvature. In the kinematic limit, the distribution of the field strength is an expanding lognormal, while that of the field-line curvature K is stationary and has a power tail $\sim K^{-13/7}$. The field strength and curvature are anticorrelated, i.e. the growing fields are mostly flat, while the sharply curved fields remain relatively weak. The field, therefore, settles into a reduced-tension state. Numerical simulations demonstrate three essential features of the nonlinear regime. First, the total magnetic energy is equal to the total kinetic energy. Second, the intermittency is partially suppressed compared to the kinematic case, as the fields become more volume-filling and their distribution develops an exponential tail. Third, the folding structure of the field is unchanged from the kinematic case: the anticorrelation between the field strength and the curvature persists and the distribution of the latter retains the same power tail. We propose a model of back reaction based on the folding picture which reproduces all of the above numerical results.

Subject headings: galaxies: magnetic fields — ISM: magnetic fields — magnetic fields — MHD — turbulence

1. INTRODUCTION

In turbulent MHD systems where the ratio of fluid viscosity and magnetic diffusivity (the magnetic Prandtl number, $Pr = \nu/\eta$) is very large, there exists a broad range of subviscous scales available to magnetic fluctuations, but not to hydrodynamic ones. This MHD regime is encountered, for example, in such astrophysical environments as the interstellar medium and protogalactic plasmas, where Pr can be as large as 10^{14} to 10^{22} (Kulsrud 1999). Since the ratio of the resistive and viscous cutoff wave numbers is $k_\eta/k_\nu \sim Pr^{1/2}$, this gives rise to subviscous scale ranges 7 to 11 decades wide.

Since the fluid is highly conducting, the magnetic-field lines are (nearly) perfectly frozen into the fluid flow. The fluid motions, even though restricted to the scales above the viscous cutoff, can excite magnetic fluctuations at much smaller scales via stretching and folding of the field lines. This possibility was first indicated by Batchelor (1950). The weak-field (kinematic) limit has been an attractive object of analytical study since the seminal work of Kazantsev (1967). The spectral theory of the kinematic dynamo driven by a random velocity field predicts exponential growth of the magnetic energy and its accumulation at the resistive scales (see Kazantsev 1967; Kulsrud & Anderson 1992; Gruzinov, Cowley, & Sudan 1996; Schekochihin, Boldyrev, & Kulsrud 2002, and references therein). More recently, it was realized that small-scale magnetic fields generated by this “stretch-and-fold” dynamo possess a distinctive spatial *folding structure* (Fig. 1): the smallness of the field scale is

due to rapid transverse spatial oscillation of the field direction, while the field lines remain largely unbent up to the scale of the flow (Ott 1998; Kinney et al. 2000; Schekochihin et al. 2002a, — this last paper is henceforth referred to as SCMM-02).

With the dramatic increase in the reach of the numerical experiment, the nonlinear regime became increasingly amenable to detailed study. The pioneering work of Meneguzzi, Frisch, & Pouquet (1981) was in recent years followed by a number of numerical investigations (Cattaneo, Hughes, & Kim 1996; Brandenburg et al. 1996; Zienicke, Politano, & Pouquet 1998; Kinney et al. 2000; Cho & Vishniac 2000; Brandenburg 2001; Chou 2001; Brummell, Cattaneo, & Tobias 2001; Maron, Cowley, & McWilliams 2002, the latter paper henceforth abbreviated MCM-02). However, the physical difference between the $Pr = 1$ and $Pr \gg 1$ regimes is not always realized.

Another defining physical feature of the MHD regime we are considering is the absence of an externally imposed uniform magnetic field. The difference is essential. First, a fixed uniform field implies a nonzero net flux through the system. Second, in the presence of a strong such field, magnetic-field lines cannot be bent, so the physics of the subviscous-scale magnetic fluctuations is more akin to that of the scalar turbulence (cf. Cho, Lazarian, & Vishniac 2002).

In the astrophysical context, the main question has been of the impact small-scale magnetic fluctuations have on the feasibility of generating the large-scale galactic magnetic field by means of turbulent dynamo. In particular, one wonders how the accumulated small-scale magnetic energy affects the applica-

bility of the mean-field $\alpha\Omega$ -dynamo theory, which, in one form or another, has been at the center of all attempts to build a theoretical understanding of the galactic magnetic fields (Beck et al. 1996). This issue remains unresolved in both the theoretical and numerical senses of the word. We note that, because of the large scale separations that have to be captured, the brute-force numerical solution of this problem remains beyond the capacity of currently available computational resources. On the other hand, the physics of the small-scale magnetic turbulence can be effectively studied as a separate problem and accessed (if only just) by numerical experiment. We hope that by developing a thorough physical understanding of the small-scale magnetic fluctuations, we can approach the problem of their interplay with the large-scale fields and motions.

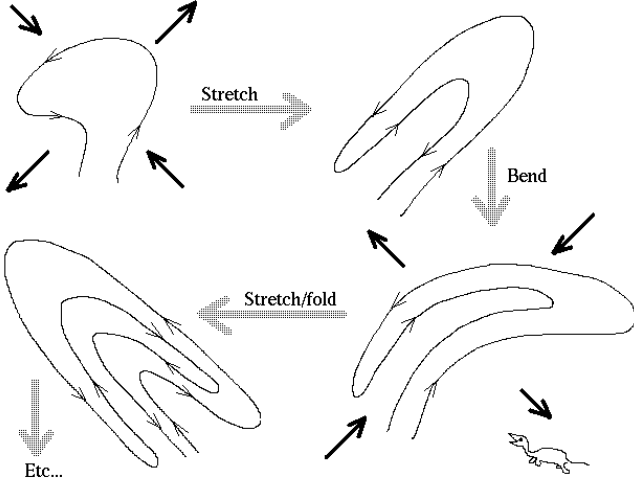


FIG. 1.— A cartoon of the folding-structure formation via stretching of the field lines. Bold arrows indicate directions in which volumes are deformed by random shear.

In this work, we concentrate on the structural properties of the small-scale magnetic fields: namely, the intermittency of their spatial distribution and the geometry of the field lines. Quantitatively, these are studied in terms of the one-point statistics of the field strength and of the field-line curvature.

We consider the nonlinear turbulent dynamo to be described by the equations of incompressible MHD:

$$\frac{d}{dt} \mathbf{u} = \nu \Delta \mathbf{u} - \nabla p + \mathbf{B} \cdot \nabla \mathbf{B} + \mathbf{f}, \quad (1)$$

$$\frac{d}{dt} \mathbf{B} = \mathbf{B} \cdot \nabla \mathbf{u} + \eta \Delta \mathbf{B}, \quad (2)$$

where $d/dt = \partial_t + \mathbf{u} \cdot \nabla$ is the convective derivative, $\mathbf{u}(t, \mathbf{x})$ is the velocity field, $\mathbf{B}(t, \mathbf{x})$ is the magnetic field, and $\mathbf{f}(t, \mathbf{x})$ is a random (white in time) large-scale forcing. The density ρ of the plasma is taken to be constant. The incompressibility condition $\nabla \cdot \mathbf{u} = 0$ is, therefore, added to the equations above and serves to determine (or, indeed, to define) pressure. For the sake of convenience, the pressure p and the magnetic field \mathbf{B} have been normalized to ρ and $(4\pi\rho)^{1/2}$, respectively.

The plan of further proceedings is as follows. In Sec. 2, we review the necessary facts about the kinematic regime of the dynamo. These are important, for they form the basis of our understanding of the dynamo and remain surprisingly relevant in the nonlinear regime. The latter constitutes our main object of study. In Sec. 3, we describe the results of our numerical experiments and propose a heuristic physical model that explains these results. Conclusions are drawn in Sec. 4.

2. THE KINEMATIC REGIME

In the weak-field (kinematic) limit, MHD turbulence reduces to the problem of passive advection of a vector field by a turbulent velocity field. The magnetic energy grows exponentially and the small-scale folding structure is formed at the time scale associated with the eddies that turn over the fastest (i.e., in Kolmogorov turbulence, the viscous-scale eddies). Physically, this follows from the fact that the turbulent eddies act on the small-scale fields as a sequence of random linear-shear transformations (see Fig. 1 and § 2.3). An expanding *lognormal* distribution of the field strength emerges, which is qualitatively explained in terms of the Central Limit Theorem.

2.1. The Kazantsev–Kraichnan Model

All of the above results can be derived analytically in the framework of the Kraichnan (1968) model of passive advection, which replaces the turbulent velocity with a Gaussian random field δ -correlated in time:

$$\langle u^i(t, \mathbf{x}) u^j(t', \mathbf{x}') \rangle = \delta(t - t') \kappa^{ij}(\mathbf{x} - \mathbf{x}'). \quad (3)$$

In the context of the small-scale dynamo, this model was first proposed by Kazantsev (1967). While the Kazantsev–Kraichnan velocity field is, of course, highly artificial and does not approximate the real turbulent velocity field in any controlled sense, its performance in capturing the essential qualitative and, in some cases, also quantitative, features of the passive advection has been very impressive (on the passive scalar, see recent review by Falkovich, Gawędzki, & Vergassola 2001; on the kinematic dynamo, see Kinney et al. 2000, SCMM-02, MCM-02, Schekochihin et al. 2002b). This seems to suggest that the statistics of passive advection may be largely universal with respect to the structure of the ambient random flow.

In the limit of large Pr , the magnetic fluctuations are mostly excited deep in the subviscous range, where the fluid motions are strongly damped by viscous dissipation. The velocity field “seen” by the magnetic field is, therefore, regular and, in fact, effectively constitutes a *single-scale flow*. Most of the relevant statistical results turn out to depend just on the first few coefficients of the Taylor expansion of the velocity correlation tensor:

$$\begin{aligned} \kappa^{ij}(\mathbf{y}) = & \kappa_0 \delta^{ij} - \frac{1}{2} \kappa_2 \left(y^2 \delta^{ij} - \frac{1}{2} y^i y^j \right) \\ & + \frac{1}{4} \kappa_4 y^2 \left(y^2 \delta^{ij} - \frac{2}{3} y^i y^j \right) + \dots \end{aligned} \quad (4)$$

(some of the coefficients in the expansion are fixed by the incompressibility constraint). Physically, $\kappa_2 \sim k_\nu u$ is the stretching rate, while κ_4 sets the scale of the flow ($\kappa_4/\kappa_2 \sim k_\nu^2$) and is responsible for bending the field lines.

2.2. Intermittency

One of the simplest and most basic features of the kinematic diffusion-free regime is the lognormality of the distribution of the magnetic-field strength (see, e.g., Boldyrev & Schekochihin 2000, SCMM-02). On the most fundamental level, the lognormal character of the distribution of B follows already from the form of the induction equation (2) (without the diffusion term). Indeed, it is linear with respect to the magnetic field, which is multiplied by a random externally prescribed velocity-gradient matrix $\nabla \mathbf{u}$. The Gaussianity of $\log B$ then follows by the Central Limit Theorem.

Within the framework of the Kazantsev–Kraichnan model, this result can be derived exactly. The one-point PDF of the magnetic-field strength in the diffusion-free regime can easily be shown to satisfy the following Fokker–Planck equation:

$$\partial_t P = \frac{1}{4} \kappa_2 \frac{\partial}{\partial B} B^4 \frac{\partial}{\partial B} \frac{1}{B^2} P. \quad (5)$$

Eq. (5) written in log variables is simply a 1D diffusion equation with a drift and has the following Green’s-function solution:

$$P(t, B) = \frac{e^{-(1/2)\kappa_2 t}}{\sqrt{\pi\kappa_2 t}} \int_0^\infty \frac{dB'}{B'} P_0(B') \times \exp\left(-\frac{[\ln(B/B') - (1/4)\kappa_2 t]^2}{\kappa_2 t}\right), \quad (6)$$

where $P_0(B)$ is the initial distribution. The lognormality means that the PDF develops considerably spread-out tails at both large and small values of B , i.e., the fluctuating magnetic fields in the kinematic regime possess a high degree of intermittency. The moments $\langle B^n \rangle$ of the magnetic field have growth rates that increase quadratically with n : $\langle B^n \rangle \propto \exp[n(n+3)\kappa_2 t/4]$. The exponential growth of the moments of B is the manifestation of the dynamo action of the turbulence. It measures the effect of stretching of the field lines by the ambient random flow.

Note that these results apply to the diffusion-free situation (i.e., to an ideally conducting medium), and, therefore, hold during the time it takes the magnetic excitation to propagate from the velocity scales, where it is assumed to be initially concentrated, to the resistive scales. This process occurs exponentially fast (Kulsrud & Anderson 1992; Schekochihin, Boldyrev, & Kulsrud 2002), so the corresponding time can be estimated as $t \sim \kappa_2^{-1} \log \text{Pr}^{1/2}$, which amounts to several eddy-turnover times. The PDF of B with account taken of diffusion has not as yet been found, though Chertkov et al. (1999) did, under certain additional assumptions, derive the moments $\langle B^n \rangle$ in the diffusive regime. While the specific expressions for the growth rates of the moments are substantially modified, they still increase as n^2 , as would be the case for a lognormal distribution, so the intermittency is not diminished.

2.3. The Folding Structure

The geometry of the magnetic-field lines can be studied in terms of the statistics of their curvature $\mathbf{K} = \hat{\mathbf{b}} \cdot \nabla \hat{\mathbf{b}}$ (here $\hat{\mathbf{b}} = \mathbf{B}/B$). The evolution equation for the curvature can be derived from the induction equation:

$$\begin{aligned} \frac{d}{dt} \mathbf{K} = & \mathbf{K} \cdot (\nabla \mathbf{u}) \cdot (\hat{\mathbf{I}} - \hat{\mathbf{b}}\hat{\mathbf{b}}) - \hat{\mathbf{b}}\hat{\mathbf{K}}\hat{\mathbf{b}} : \nabla \mathbf{u} - 2\hat{\mathbf{K}}\hat{\mathbf{b}}\hat{\mathbf{b}} : \nabla \mathbf{u} \\ & + \hat{\mathbf{b}}\hat{\mathbf{b}} : (\nabla \nabla \mathbf{u}) \cdot (\hat{\mathbf{I}} - \hat{\mathbf{b}}\hat{\mathbf{b}}), \end{aligned} \quad (7)$$

where we have dropped diffusion terms. For the Kazantsev–Kraichnan velocity, the PDF of curvature satisfies the following Fokker–Planck equation (SCMM-02)

$$\partial_t P = \frac{7}{4} \kappa_2 \frac{\partial}{\partial K} K \left[\left(1 + K^2\right) \frac{\partial}{\partial K} \frac{1}{K} P + \frac{20}{7} P \right], \quad (8)$$

where K has been rescaled by $K_* = (12\kappa_4/7\kappa_2)^{1/2} \sim k_\nu$. From this equation one immediately finds that the curvature attains a stationary distribution:

$$P(K) = \frac{7}{5} \frac{K}{(1 + K^2)^{10/7}}. \quad (9)$$

This PDF has a power tail $\sim K^{-13/7}$, which is in very good agreement with numerics (SCMM-02). Naturally, if the resistive regularization is introduced, the power tail is cut off at

$K \sim k_\eta \sim \text{Pr}^{1/2} k_\nu$. The bulk of the curvature distribution is concentrated at values of curvature $K \sim k_\nu$, which reflects the prevailing straightness of the field lines at subviscous scales. The field lines are significantly curved only in the bends of the folds. While these bends occupy a small fraction of the volume, there is a high degree of intermittency in the distribution of the characteristic scales associated with them. This is reflected by the power tail of the curvature PDF.

Furthermore, *the field strength and the curvature are anticorrelated*, i.e. the growing fields are mostly flat, while the curved fields in the bends of the folds remain relatively weak. It is not hard to realize that the nature of this anticorrelation, which is derived as a statistical property in SCMM-02, is, in fact, dynamical. Since this fact will be important in our discussion of the nonlinear back reaction in § 3.2, we would like to explain it in more detail.

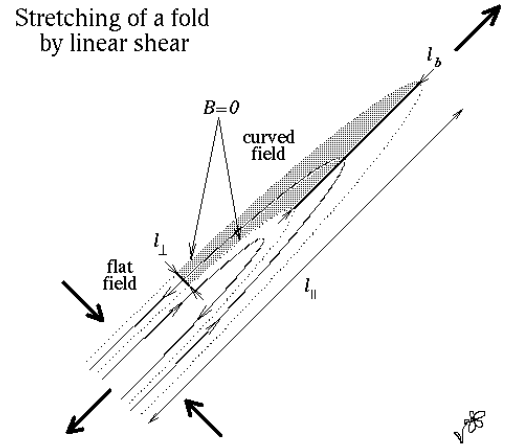


FIG. 2.— A cartoon of the stretching of a fold by linear shear. The bold arrows indicate the action of the shear. The dotted lines correspond to surfaces where $B = 0$. The shaded area is the cross-section of the volume used for the flux-conservation estimate (10): all the flux is through the surfaces whose cross-sections are represented by bold lines.

Consider what happens when a typical element of the folding structure (Fig. 2) is stretched by linear shear. Let B_f and K_f be the magnetic-field strength and curvature associated with the flat part of the fold, and B_b and K_b their counterparts in the curved part (the bend). Also let l_\parallel be the length of the fold (parallel scale of the field), l_\perp its thickness (perpendicular scale of the field), and l_b the length of the bend. Then, by flux conservation within the volume indicated by the shaded area in Fig. 2, we must have

$$B_f l_\perp \sim B_b l_b. \quad (10)$$

Suppose that the fold is stretched by a factor s in the parallel direction. Then $l_\parallel \rightarrow s l_\parallel$, $l_b \rightarrow s l_b$, and, by volume and flux conservation, $l_\perp \rightarrow (1/s) l_\perp$, $B_f \rightarrow s B_f$, so the field is amplified in the flat part of the fold. Using Eq. (10), we then get $B_b \sim (l_\perp/l_b) B_f \rightarrow (1/s) B_b$, so the field in the bend is weakened. We now observe that $K_f \sim 1/l_\parallel$ and $K_b \sim 1/l_\perp$, which implies that, during stretching, $K_f \rightarrow (1/s) K_f$ and $K_b \rightarrow s K_b$. We conclude that linear shear transformation preserves

$$KB \sim \text{const} \quad (11)$$

throughout the fold. Hence the anticorrelation between B and K .

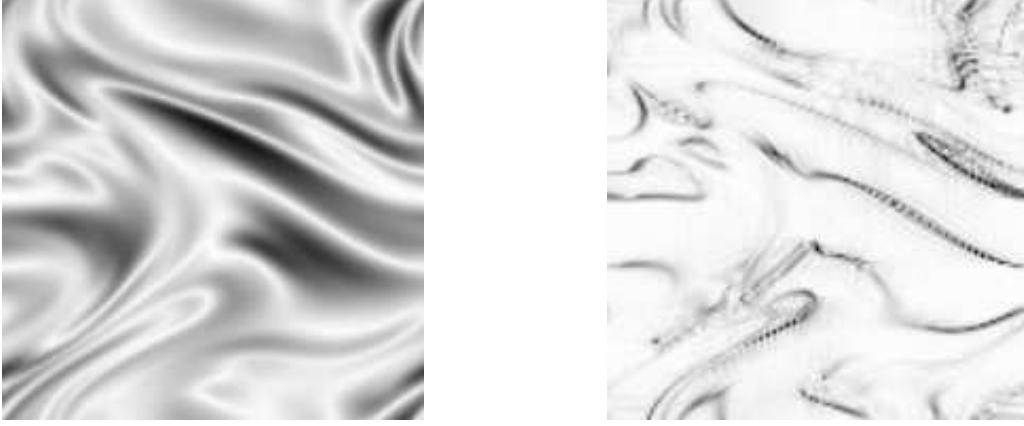


FIG. 3.— Instantaneous cross-sections of the field strength B (left) and curvature K (right) during the nonlinear stage of a simulation with $\nu = 5 \cdot 10^{-2}$, $\eta = 2 \cdot 10^{-4}$ ($\text{Pr} = 250$). Darker areas correspond to larger values. Detailed anticorrelation between B and K is manifest.

The perceptive reader might wonder about the consistency of Eq. (11) with our previously stated results that, while the statistics of the field strength are lognormal, the curvature distribution has a power tail. The explanation is as follows. The argument that led to Eq. (11) was based on approximating the ambient flow by a *linear* shear and thus described the effect of the first derivatives of the velocity on the magnetic field. We now observe that the curvature evolution equation (7) also contains the second derivatives of velocity, which enter as a source term. Their role is to *bend* the field lines at the scale of the flow (see Fig. 1): once the field becomes too flat (i.e., flatter than the flow), it is bent within one eddy-turnover time and $K \sim k_\nu$ is restored. Therefore, the curvature cannot remain below values of order k_ν for a long time (or in many places). In formal terms, the second derivatives of velocity break the scale invariance of Eq. (7) and, consequently, of the associated Fokker–Planck equation (8) (this is reflected in the presence of unity in the first term on the right-hand side). A stationary distribution with a power tail is thereby made possible. In fact, this power tail is a limiting envelope for a lognormal tail produced by the action of the linear shear (see SCMM-02).

The most important consequence is that the field settles into a *reduced-tension state*: the tension force can be estimated by $\mathbf{B} \cdot \nabla \mathbf{B} \sim k_\parallel B^2 \sim KB^2 \sim k_\nu B^2$ on the average. A simple *reductio ad absurdum* argument can be envisioned to further support this statement. Let us write the evolution equation for $\mathbf{F} = \mathbf{B} \cdot \nabla \mathbf{B}$:

$$\frac{d}{dt} \mathbf{F} = \mathbf{F} \cdot \nabla \mathbf{u} + \mathbf{B} \mathbf{B} : \nabla \nabla \mathbf{u}, \quad (12)$$

where the diffusion terms are again dropped. Suppose for a moment that the field is chaotically tangled, i.e. $F \sim k_\parallel B^2$ with $k_\parallel \sim k_\perp \gg k_\nu$. Then the term in Eq. (12) that involves the second derivatives of the velocity field can be neglected and Eq. (12) becomes formally identical to the evolution equation for \mathbf{B} . The moments of \mathbf{F} must, therefore, grow at the same rates as the moments of \mathbf{B} , and we estimate $\langle F^2 \rangle / \langle B^4 \rangle \propto \langle B^2 \rangle / \langle B^4 \rangle$, which decays exponentially fast in time. An exact statistical calculation for the Kazantsev–Kraichnan velocity, shows that, indeed,

$$\frac{\langle |\mathbf{B} \cdot \nabla \mathbf{B}|^2 \rangle}{\langle B^4 \rangle} \rightarrow \frac{28}{9} \frac{\kappa_4}{\kappa_2} \sim k_\nu^2 \quad (13)$$

asymptotically with time, starting from any initial conditions (SCMM-02). The convergence is exponentially fast at the stretching (eddy-turnover) rate. We conclude that even an ini-

tially chaotically tangled magnetic field will quickly develop the folding structure.

Thus, the nonlinear saturation, which is due to the Lorentz tension balancing the stretching action of the flow, occurs when the energy of the field becomes comparable to the energy of the turbulent eddies. Note that in the hypothetical chaotically tangled field with $k_\parallel \sim k_\perp$, the tension would be much larger: $\mathbf{B} \cdot \nabla \mathbf{B} \sim k_\eta B^2$, so saturation would be possible already at very low magnetic energies.

3. THE NONLINEAR REGIME

3.1. Numerical Results

No satisfactory analytical description of the nonlinear state is as yet available, so one must be guided by results of numerical experiments. The main obstacle in the way of a definitive numerical study is the tremendously wide range of scales that must be resolved in order to adequately simulate the large- Pr MHD: indeed, one must resolve *two* scaling intervals, the hydrodynamic inertial range and the subviscous magnetic one. Since this is not feasible, we propose to simulate the initial stage of the nonlinear evolution up to the point when the *total* energy of the magnetic field equalizes with the energy of the viscous-scale turbulent eddies. This stage can be studied in the *viscosity-dominated MHD regime* where the hydrodynamic Reynolds number Re is order one and the external forcing models the energy supply from the larger eddies (cf. Cattaneo, Hughes, & Kim 1996; Kinney et al. 2000). Moreover, one can argue (MCM-02) that once the magnetic energy does equalize with that of the smallest eddies, the following scenario takes place. The magnetic back reaction leads to suppression of the shearing motions associated with the viscous-scale eddies. Larger-scale eddies, which are more energetic (but have slower turnover rates), continue to drive the small-scale magnetic fluctuations until the latter become strong enough to suppress these eddies as well. This process continues until the entire inertial range is suppressed, so *the system asymptotes to a state where the energy received by the outer-scale eddies from the external forcing is transferred directly into the small-scale magnetic fluctuations*. Speculatively, this could be thought of as some effective renormalization of Re , so that the final statistics of the magnetic field would again be described by the low- Re MHD model. Some numerical evidence supporting this picture is given by MCM-02.

In our simulations, we choose $\text{Re} = \nu^{-1} = 20$, so the forcing and the viscous scales are comparable and the statistics of the subviscous-range magnetic fluctuations can be studied already at 128^3 resolution. The numerical set-up and the spectral MHD code used are exhaustively described in MCM-02.

After the initial kinematic growth stage, saturation is achieved where the total magnetic and hydrodynamic energies are equal.¹ We then measure the PDFs of the magnetic-field strength and curvature in the saturated state. Our findings are as follows.

(1) *The level of intermittency is lower than in the kinematic case, the field-strength distribution developing an exponential tail.* The kurtosis of the field decreases to $\langle B^4 \rangle / \langle B^2 \rangle^2 \sim 4$ after growing exponentially during the kinematic stage.

The partial suppression of intermittency indicates a plausible scenario for the onset of nonlinearity (see Fig. 4). As we saw in § 2.2, the kinematic dynamo gives rise to a highly intermittent lognormal spatial distribution of the field strength. Already early on, when the total magnetic energy is only a fraction of its saturated value, there are tiny regions where the magnetic-energy density locally approaches values comparable to, and greater than, the energy density of the fluid motions. This activates the nonlinear back reaction in these regions, so as to suppress further growth of the field there. As the overall amount of the magnetic energy grows, the fraction of the volume where the nonlinearity is at work increases until the nonlinear state is established globally. In the process, the magnetic fields become more volume-filling and, consequently, less intermittent (cf. Brandenburg et al. 1996; Cattaneo 1999a,b).

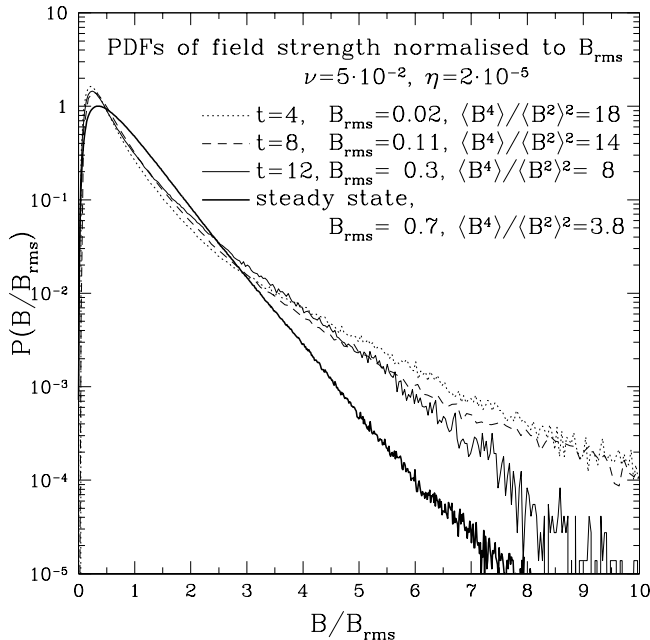


FIG. 4.— PDFs of the field strength: onset of nonlinearity and saturation. The field strength is normalized to its rms value for each PDF. The intermittency at earlier times is thus clearly seen to be stronger than during the saturated stage.

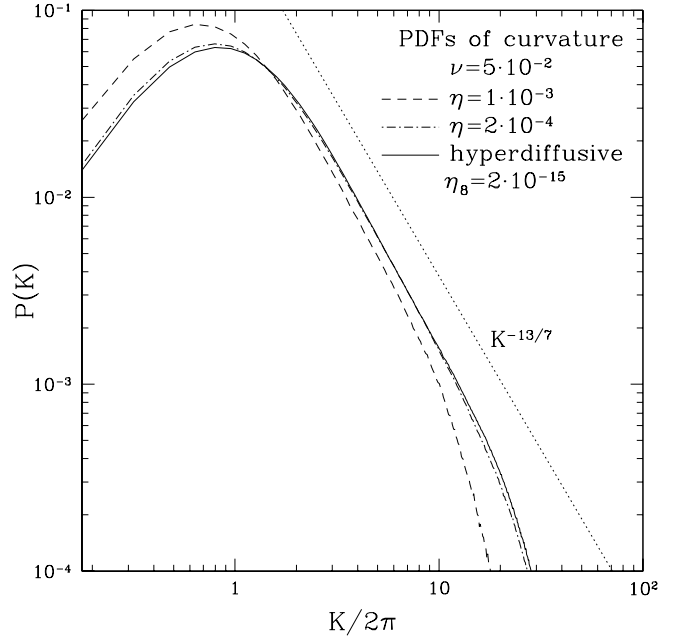


FIG. 5.— PDFs of the field-line curvature in the nonlinear regime. The solid curve is for a simulation that used 8th-order hyperdiffusion. At curvatures approaching resistive cutoff, $K \sim k_\eta$, the scaling is destroyed.

(2) *The folding structure of the field is unchanged from the kinematic case.* The anticorrelation between the field strength and the curvature persists (see Fig. 3, which illustrates the dynamical nature of this anticorrelation discussed in § 2.3). Their correlation coefficient $r_{K,B} = \langle K^2 B^2 \rangle / \langle K^2 \rangle \langle B^2 \rangle - 1 \sim -0.7$ in our simulations, which is quite close to its minimum allowed value of -1 . Even more remarkably, the distribution of the curvature retains the same power tail $\sim K^{-13/7}$ (Fig. 5). We find this last feature particularly striking: indeed, not only does a kinematic theory based on the synthetic Kraichnan velocity field predict a quantitatively correct nontrivial scaling for the tail of the curvature PDF, but this scaling also survives in the fully nonlinear case!

Finally, we would like to offer the following caveat with regard to the numerical study of the small-scale magnetic turbulence by means of spectral methods. We have found that if the amount of dissipation applied to the magnetic field is not sufficiently large to completely override the effect of dealiasing (see Canuto et al. 1988), the folding structure is destroyed and incorrect curvature statistics are obtained (cf. MCM-02). The resulting resolution constraints tend to be quite stringent: it is not enough to simply make sure that the UV cutoff of magnetic-energy spectrum is resolved. We believe that the destruction of the structural properties of the field by dealiasing is due to non-local nature of the corresponding operator. Consistently with this view, hyperdiffusion does not exhibit the same adverse effect (see Fig. 5).

3.2. A Model of Back Reaction

The physical reason for the preservation of the folding structure is, of course, that the fluid motions at subviscous scales are strongly damped and cannot “unwrap” the folds. Here we use the folding picture to devise a simple *ad hoc* physical model that

¹ This equipartition only holds asymptotically with Pr . When the magnetic diffusivity is too large, saturation occurs at smaller magnetic energies (for more details, see Schekochihin et al. 2002b). This probably accounts for subequipartition saturated states seen in some of the simulations of small-scale dynamo (e.g., Brummell, Cattaneo, & Tobias 2001). We note, however, that the lower magnetic-energy levels in the saturated state do not alter either the intermittency- or the structure-related properties of the small-scale fields.

explains the two key quantitative results that have emerged from our numerics: the exponential tail of the PDF of the magnetic-field strength and the unchanged kinematic power tail of the curvature PDF.

It is clear that, once the magnetic fields grow strong enough, they will resist further stretching by the ambient velocity shear. This increased rigidity of the field can be modelled by adding a nonlinear relaxation term to the induction equation:

$$\frac{d}{dt} \mathbf{B} = \mathbf{B} \cdot \nabla \mathbf{u}_{\text{ext}} - \tau_r^{-1}(B) \mathbf{B}, \quad (14)$$

where \mathbf{u}_{ext} is the part of the velocity field due to the external forcing and $\tau_r(B)$ is some effective nonlinear relaxation time.²

In view of the heuristic way in which the nonlinearity has been introduced into the induction equation, Eq. (14) *cannot* be expected to, and, indeed, does not, correctly model the spatial properties of the magnetic field. What it effectively amounts to is a simple *local* one-point closure. If the external velocity field is modelled by the Kazantsev–Kraichnan velocity, the Fokker–Planck equation (5) derived in the kinematic case can easily be amended to include the nonlinearity:

$$\partial_t P = \frac{\partial}{\partial B} B \left[\frac{1}{4} \kappa_2 B^3 \frac{\partial}{\partial B} \frac{1}{B^2} P + \tau_r^{-1}(B) P \right]. \quad (15)$$

This equation has one normalizable stationary solution

$$P(B) = \text{const} B^2 \exp \left[-\frac{4}{\kappa_2} \int_0^B \frac{dB'}{B'} \tau_r^{-1}(B') \right]. \quad (16)$$

In order to make an intelligent guess about the B -dependence of $\tau_r^{-1}(B)$, we have to invoke our understanding of the field structure at subviscous scales. The relaxation term in Eq. (14) is due to the suppression of the velocity shear by the Lorentz back reaction. The latter can be thought of as inducing a certain magnetic component \mathbf{u}_m of the velocity field which counterbalances the external shear, so $\tau_r^{-1}(B) \sim \nabla \mathbf{u}_m$. Since we are considering a viscosity-dominated regime, $\nabla \mathbf{u}_m$ should be estimated by balancing the viscous damping and the magnetic tension:

$$-\nu \Delta \mathbf{u}_m \sim \mathbf{B} \cdot \nabla \mathbf{B}. \quad (17)$$

The characteristic scale of \mathbf{u}_m cannot be smaller than the viscous scale: otherwise, \mathbf{u}_m would be viscously damped at a shorter time scale than that of the external shear and could not provide an effective counteraction to it. We have, therefore,

$$\tau_r^{-1}(B) \sim k_\nu u_m \sim \frac{\mathbf{B} \cdot \nabla \mathbf{B}}{\nu k_\nu} \sim \frac{KB^2}{\nu k_\nu}. \quad (18)$$

We emphasize that the above relation represents a *local* force balance in a particular fold. Now, in a *typical* case, the folding structure would imply $K \sim k_\nu$, so

$$\tau_r^{-1}(B) \sim \frac{B^2}{\nu}, \quad B \sim B_{\text{typical}}, \quad (19)$$

where $B_{\text{typical}} \sim B_{\text{rms}}$ is the typical value of the back-reacting magnetic field in the system. This regime corresponds to what is sometimes referred to as the *viscous relaxation effect* (Chandran 1997; Kinney et al. 2000). Substituting the expression (19) for $\tau_r^{-1}(B)$ into Eq. (16), we find a Gaussian PDF (cf. Boldyrev 2001) with $B_{\text{rms}} \sim (\kappa_2 \nu)^{1/2}$, which approximately corresponds to magnetic energy equalizing with the energy of the viscous-scale eddies and accounts for the energy equipartition we have seen in our simulations.

However, these arguments are only appropriate in application to the statistics of the *typical* values of the magnetic-field strength, i.e., to the *core* of the distribution function (cf. Boldyrev 2001). In order to understand the *tail* of the PDF, one must consider *rare* events, specifically, the instances (or places) where B is *atypically large*. In the framework of the “stretch-and-fold” small-scale dynamo mechanism, such events can occur if magnetic field gets “overstretched” (say, because the shear has acted coherently in one direction for an atypically long time). The local relation between the curvature and the field strength associated with it is given by Eq. (11), whence $KB \sim k_\nu B_{\text{typical}}$. Inserting this into Eq. (18), we find

$$\tau_r^{-1}(B) \sim \frac{BB_{\text{typical}}}{\nu}, \quad B \gg B_{\text{typical}}, \quad (20)$$

which, upon substitution into Eq. (16), gives the exponential tail evidenced by the numerics.

The persistence of the kinematic curvature statistics in the face of nonlinear effects can also be understood in these terms. Essentially, the tail of the curvature PDF remains unaffected by the back reaction because it describes areas of anomalously large curvature ($K \gg k_\nu$) where, due to the anticorrelation property, the field is weak. On a slightly more quantitative level, we argue that the effect of the back reaction on the curvature can also be modelled by a simple nonlinear relaxation term, as in Eq. (14):

$$\frac{d}{dt} \mathbf{K} = [\text{rhs of Eq. (7) with } \nabla \mathbf{u}_{\text{ext}}] - \tau_r^{-1}(B) \mathbf{K}. \quad (21)$$

Here $\tau_r^{-1}(B)$ is again estimated via Eqs. (18) and (11). The nonlinear relaxation term in Eq. (21) is then

$$-\tau_r^{-1}(B) \mathbf{K} \sim -\frac{(KB)^2}{\nu k_\nu} \hat{\mathbf{n}} \sim -\frac{k_\nu B_{\text{typical}}^2}{\nu} \hat{\mathbf{n}}, \quad (22)$$

where $\hat{\mathbf{n}} = \mathbf{K}/K$. With this correction, the Fokker–Planck equation (8) for the PDF of curvature becomes

$$\partial_t P = \frac{7}{4} \kappa_2 \frac{\partial}{\partial K} K \left[(1+K^2) \frac{\partial}{\partial K} \frac{1}{K} P + \frac{20}{7} P - \frac{\alpha}{K} P \right], \quad (23)$$

where α is a numerical constant of order unity and, as before, K is rescaled by $K_* \sim k_\nu$. It is a straightforward exercise to show that the stationary PDF is now given by

$$P(K) = \text{const} \frac{K e^{\alpha \arctan(K)}}{(1+K^2)^{10/7}}, \quad (24)$$

which has the same power tail $\sim K^{-13/7}$ as its kinematic counterpart (9).

Finally, we would like to stress the qualitative character of the ideas and results put forward in this section. A more quantitative nonlinear theory based on these ideas may be feasible, but is left for future work. Another important issue that requires careful quantitative treatment is the role of Ohmic diffusion. Based on the model of back reaction proposed here, we seem to be able to understand the nonlinear regime without including the resistive terms. These terms are hard to treat analytically due to the usual closure problem associated with the diffusion operator. Numerically, we have confirmed that the field structure is unaffected by a switch to hyperdiffusion (see Fig. 5), but the locality of the dissipation operator probably does matter (see remarks at the end of § 3.1). Further investigation of the universality of the statistics of the small-scale magnetic turbulence with respect to the form of the UV regularization is also left for the future.

² A model of nonlinear feedback mathematically very similar to this one was studied by Zeldovich et al. (1987) in the problem of self-excitation of a nonlinear scalar field in a random medium.

4. CONCLUSIONS

We have found that the folding structure of subviscous-scale magnetic fluctuations that is formed via the kinematic “stretch-and-fold” small-scale-dynamo mechanism remains the essential feature of the nonlinear regime. The scale separation is of crucial importance here: while small-scale structure can be generated and maintained in large-scale random flows, these flows lack the ability to coherently undo the structure even when acting in concert with the magnetic back reaction.

Both our theoretical arguments and our numerical experiments were based on viewing the turbulent velocity field as a single-scale random flow. In real turbulence, Re is, of course, fairly large (10^4 in the ISM), so many hydrodynamic scales come into play. Unfortunately, the resulting scale ranges are too broad to be adequately simulated. It is interesting, however, that the results presented above appear to hold in simulations with more realistic Re (up to 10^3) but relatively small Pr (down to values of order one), in accordance with the arguments presented at the beginning of Sec. 3. We believe, therefore, that the physics and the numerics we have laid out provide at least a semiquantitative description of the statistical properties of the small-scale MHD turbulence in high- Pr plasmas.

The implications for astrophysical objects can be significant. For the large-scale galactic dynamo, small-scale fields must be taken into consideration if a nonlinear $\alpha\Omega$ theory is to be constructed. If the net effect of the accumulated small-scale magnetic energy is to suppress α , an alternative theory will have to be sought. In the accretion-disk physics, presence of large amounts of small-scale magnetic energy could lead to new models for the angular-momentum transport (Balbus & Hawley 1998) and for the acceleration of jets (see, e.g., Heinz & Begelman 2000). In the solar astrophysics, the possibility was recently raised that a substantial part of the magnetic energy in the quiet photosphere of the Sun resides in small-scale magnetic fluctuations (Cattaneo 1999b). Indeed, it is natural to expect that, just as turbulence itself, small-scale random magnetic fields are ubiquitous in the Universe.

Finally, constructing a self-consistent physical theory of the

small-scale magnetic turbulence constitutes a fascinating task in its own right. Though fifty years have passed since Batchelor (1950) took the first steps down this road, an inquisitive researcher will still find surprises at every turn, and it might well be short-sighted to claim that we are able to discern the contours of the final destination.

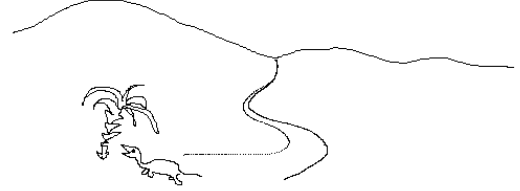


FIG. 6.— The road ahead.

It is a pleasure to thank E. Blackman, S. Boldyrev, W. Dorland, P. Goldreich, G. Hammett, R. Kulsrud, L. Malyskin, A. Shukurov, and D. Uzdensky for stimulating discussions. Our work was supported by the UKAEA Agreement No. QS06992, the EPSRC Grant No. GR/R55344/01, the NSF Grants No. AST 97-13241 and AST 00-98670, and the USDOE Grant No. DE-FG03-93ER54 224. Simulations were run on the supercomputers of the National Center for Supercomputing Applications (NCSA) and of the UK Astrophysical Fluids Facility (UKAFF).

REFERENCES

- Balbus, S. A. & Hawley, J. F. 1998, *Rev. Mod. Phys.*, 70, 1
 Batchelor, G. K. 1950, *Proc. Roy. Soc. London, Ser. A*, 201, 405
 Beck, R., Brandenburg, A., Moss, D., Shukurov, A., & Sokoloff, D. 1996, *ARA&A*, 34, 155
 Boldyrev, S. A. 2001, *ApJ*, 562, 1081
 Boldyrev, S. A. & Schekochihin, A. A. 2000, *Phys. Rev. E*, 62, 545
 Brandenburg, A. 2001, *ApJ*, 550, 824
 Brandenburg, A., Jennings, R. L., Nordlund, A., Rieutord, M., Stein, R. F., & Tuominen, I. 1996, *J. Fluid Mech.*, 306, 325
 Brummell, N. H., Cattaneo, F., & Tobias, S. M. 2001, *Fluid Dyn. Res.*, 28, 237
 Canuto, C., Hussaini, M. Y., Quarteroni, A., & Zang, T. A. 1988, *Spectral Methods in Fluid Dynamics* (Berlin: Springer)
 Cattaneo, F. 1999a, in: *Motions in the Solar Atmosphere*, ed. A. Hansmeier & M. Messerotti (Dordrecht: Kluwer), 119
 Cattaneo, F. 1999b, *ApJ*, 515, L39
 Cattaneo, F., Hughes, D. W., & Kim, E. 1996, *Phys. Rev. Lett.*, 76, 2057
 Chandran, B. D. G. 1997, *ApJ*, 492, 179
 Chertkov, M., Falkovich, G., Kolokolov, I., & Vergassola, M. 1999, *Phys. Rev. Lett.*, 83, 4065
 Cho, J., Lazarian, A., & Vishniac, E. T. 2002, *ApJ*, 566, L49
 Cho, J. & Vishniac, E. T. 2000, *ApJ*, 538, 217
 Chou, H. 2001, *ApJ*, 556, 1038
 Falkovich, G., Gawędzki, K., & Vergassola, M. 2001, *Rev. Mod. Phys.*, 73, 913
 Gruzinov, A., Cowley, S., & Sudan, R. 1996, *Phys. Rev. Lett.*, 77, 4342
 Heinz, S. & Begelman, M. C. 2000, *ApJ*, 535, 104
 Kazantsev, A. P. 1967, *Zh. Eksp. Teor. Fiz.*, 53, 1806 (*Sov. Phys. JETP*, 26, 1031)
 Kinney, R. M., Chandran, B., Cowley, S., & McWilliams, J. C. 2000, *ApJ*, 545, 907
 Kraichnan, R. H. 1968, *Phys. Fluids*, 11, 945
 Kulsrud, R. M. 1999, *ARA&A*, 37, 37
 Kulsrud, R. M. & Anderson, S. W. 1992, *ApJ*, 396, 606
 Maron, J., Cowley, S., & McWilliams, J. 2002, preprint (astro-ph/0111008); *ApJ*, submitted (MCM-02)
 Meneguzzi, M., Frisch, U., & Pouquet, A. 1981, *Phys. Rev. Lett.*, 47, 1060
 Ott, E. 1998, *Phys. Plasmas*, 5, 1636
 Schekochihin, A. A., Boldyrev, S. A., & Kulsrud, R. M. 2002, *ApJ*, 567, 828
 Schekochihin, A., Cowley, S., Maron, J., & Malyskin, L. 2002a, *Phys. Rev. E*, 65, 016305 (SCMM-02)
 Schekochihin, A. A., Maron, J. L., Cowley, S. C., & McWilliams, J. C. 2002b, “The nonlinear small-scale dynamo,” in preparation
 Zeldovich, Ya. B., Molchanov, S. A., Ruzmaikin, A. A., & Sokoloff, D. D. 1987, *Proc. Natl. Acad. Sci. USA*, 84, 6323
 Zienicke, E., Politano, H., & Pouquet, A. 1998, *Phys. Rev. Lett.*, 81, 4640